European Journal of Radiology Open 14 (2025) 100631

Contents lists available at ScienceDirect

European Journal of Radiology Open

journal homepage: www.elsevier.com/locate/ejro

Assessment of hemodynamic disturbances and impaired ventricular filling in asymptomatic fontan patients: A 4D flow CMR study

Li-Wei Hu [a,1], Xiaodan Zhao [b,1], Shuang Leng [b,c], RongZhen Ouyang [a], Qian Wang [a], Ai-Min Sun [a], Yi-Man Liu [d], Wei Dong [e], Liang Zhong [b,c,*], Yu-Min Zhong [a,**]

[a] Department of Radiology, Shanghai Children's Medical Center, Shanghai Jiao Tong University School of Medicine, 1678 Dong Fang Road, Shanghai 200127, PR China
[b] National Heart Research Institute Singapore, National Heart Centre Singapore, 5 Hospital Drive, Singapore 169609, Singapore
[c] Duke-NUS Medical School, Singapore, National University of Singapore, 8 College Road, Singapore 169857, Singapore
[d] Department of Pediatric Cardiology, Shanghai Children's Medical Center, Shanghai Jiao Tong University School of Medicine, 1678 Dong Fang Road, Shanghai 200127, PR China
[e] Department of Cardiothoracic Surgery, Shanghai Children's Medical Center, Shanghai Jiaotong University School of Medicine, 1678 Dong Fang Road, Shanghai 200127, PR China

HIGHLIGHTS

- Direct flow and residual volume may serve as indicators for assessing between asymptomatic Fontan patients and controls.
- Decreased KE parameters exhibited impaired ventricular filling in asymptomatic Fontan patients.
- The identification of direct flow as a marker for predicting diastolic dysfunction in left ventricular (LV) and biventricular (BiV) Fontan subgroups was demonstrated.
- The LV Fontan subgroup demonstrated a more efficient intracardiac flow pattern better than RV and BiV Fontan subgroups.

ARTICLE INFO

Keywords:
CMR
4D flow
Fontan
Flow component
Kinetic energy

ABSTRACT

Background: The Fontan procedure is a surgical intervention designed for patients with single ventricle physiology, wherein the systemic venous return is redirected into the pulmonary circulation, thereby facilitating passive pulmonary blood flow without the assistance of ventricular propulsion. Consequently, long-term follow-up of individuals who have undergone the asymptomatic Fontan procedure is essential.
Objectives: The aims of this investigation were to: 1) examine the impact of flow components and kinetic energy (KE) parameters on hemodynamic disturbances in asymptomatic Fontan patients and control group; 2) Assess left ventricular diastolic dysfunction through the analysis of 4D flow parameters across different Fontan sub-groups; 3) Compare intracardiac flow parameters among Fontan sub-groups based on morphological features of the left ventricle (LV) and right ventricle (RV).
Methods: Twenty-five Fontan patients (mean age: 10 ± 3 years, male/female: 15/10) and fourteen control subjects (mean age: 10 ± 2 years, male/female: 8/6) were recruited retrospectively for the study. The Fontan patients were further categorized into three groups based on their ventricular function: left ventricular (LV), right ventricular (RV), and biventricular (BiV). Each participant underwent cardiovascular magnetic resonance (CMR) imaging, including cine and 4D flow sequences on a 3.0 T scanner. Ventricular flow components and KE were

Abbreviations: 4D, Four-dimensional; 2D b-SSFP, 2D balanced steady state free precession; AUC, Area under curve; BiV, Biventricular; CMR, Cardiovascular magnetic resonance; BSA, Body surface area; CHD, Congenital heart disease; CO, Cardiac output; COV, Coefficient of variation; CPET, cardiopulmonary exercise testing; DCM, Dilated cardiomyopathy; EL, Energy loss; EDV, End-diastolic volume; ESV, End-systolic volume; EF, Ejection fraction; FSV, Functional single ventricle; ICC, intraclass correlation coefficient; KE, Kinetic energy; KEi_{EDV}, KE index ventricular end-diastolic volume; LV, left ventricle; RV, right ventricle; ROC, Receiver operator characteristic; SV, Stroke volume; $T\text{-}D_{max}$, Time to maximal displacement.

* Corresponding author at: National Heart Research Institute Singapore, National Heart Centre Singapore, 5 Hospital Drive, Singapore 169609, Singapore.
** Correspondence to: Department of Radiology, Shanghai Children's Medical Center, School of Medicine, Shanghai Jiao Tong University, 1678 Dong Fang Rd, Shanghai 200127, China.
E-mail addresses: zhong.liang@nhcs.com.sg (L. Zhong), zyumin2002@163.com (Y.-M. Zhong).
[1] Li-Wei Hu and Xiaodan Zhao had equal contribution and are joint first authors.

https://doi.org/10.1016/j.ejro.2024.100631
Received 28 September 2024; Received in revised form 9 December 2024; Accepted 27 December 2024

assessed using 4D flow. The study utilized cine images to analyze cardiac function and inter-ventricular mechanical dyssynchrony. Echocardiography evaluated functional ventricular diastolic dysfunction.
Results: Fontan patients had a higher median functional single ventricle (FSV) residual volume compared to controls (28 % vs. 23 %, P = 0.034), with lower median FSV direct flow (32 % vs. 40 %, P = 0.005) and delayed ejection flow (17 % vs. 24 %, P = 0.024). The parameters of FSV normalized to the ventricular end-diastolic volume (KEi_{EDV}) were found to be significantly lower in Fontan patients (all P < 0.05). In both left ventricle (LV) and biventricular (BiV) Fontan subgroups, direct flow was identified as an independent predictor of LV diastolic dysfunction (AUC=0.76, Sensitivity=86 %, Specificity=70 %). Furthermore, residual volume and E-wave KEi_{EDV} were observed to be significantly different between LV and right ventricle (RV) Fontan subgroups.
Conclusions: The altered flow pattern and reduced kinetic energy observed in Fontan patients may indicate hemodynamic disturbances and compromised ventricular filling. Reduced direct flow is associated with LV diastolic dysfunction in LV and BiV Fontan subgroups. Systemic LV exhibited a more efficient intracardiac flow pattern compare with systemic RV in Fontan patients.

1. Introduction

The Fontan procedure is a surgical palliative intervention for patients with single ventricle physiology, designed to redirect systemic venous return into the pulmonary circulation, thereby facilitating passive pulmonary blood flow without the need for ventricular propulsion (Fig. 1). This raises questions regarding the long-term follow-up of this non-physiologic circulation and the associated specific complications, such as liver disease, exudative enteropathy, and Fontan failure. [1]. However, patients with functional single ventricle (FSV) circulations exhibit suboptimal long-term outcomes due to the manifestation of symptoms associated with circulatory failure [2]. Diastolic ventricular dysfunction is prevalent in preserved ejection fraction Fontan patients [3,4]. Impaired ventricular filling and increased ventricular afterload are obvious contributors to cardiac inefficiency. Long-term follow-up of individuals who have undergone the asymptomatic Fontan procedure is essential for early detection of heart failure, Intracardiac hemodynamic changes may serve as a valuable non-invasive imaging marker for the assessment of asymptomatic Fontan patients [5].

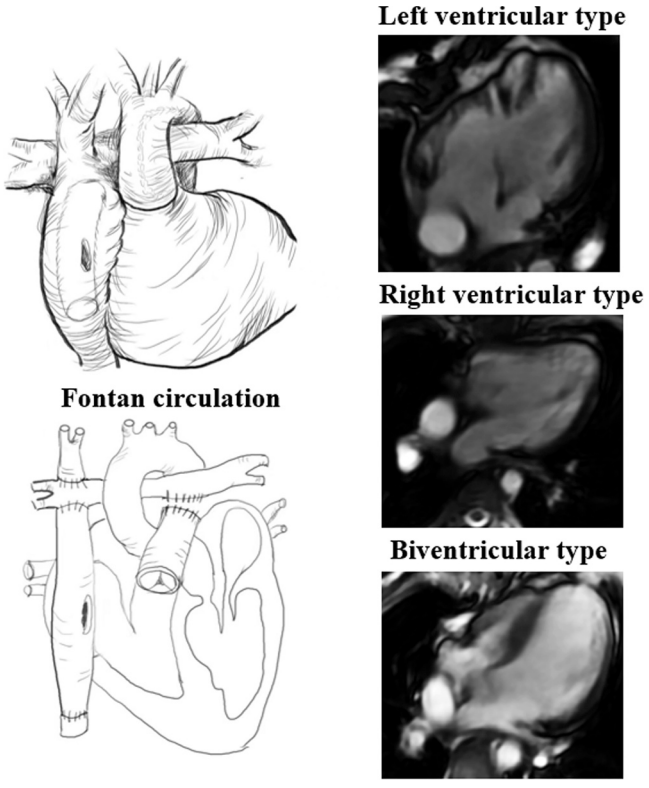

Fig. 1. Diagram of the physiological anatomy with extracardiac modification of the Fontan procedure and subgroup. The extracardiac lateral tunnel Fontan involves the right ventricle as the main pumping chamber responsible for systemic circulation.

The conventional echocardiography imaging modality is constrained in its ability to analyze intracardiac hemodynamics due to its primary dependence on two-dimensional planar flow data [6]. Four-dimensional flow (4D flow) cardiovascular magnetic resonance (CMR) can retrospectively measure intra and extracardiac great vessels blood flow draining in and out of the heart [7–9].4D flow CMR provide a detailed information about the three-directional velocities which can capture complex intracardiac of blood flow in congenital heart disease (CHD) [10]. Moreover, intracardiac flow analysis by 4D flow CMR could assess higher-order fluid dynamic metrics such as kinetic energy (KE) [11] and viscous energy loss (EL) in FSV patients [12]. Previously, some authors reported ventricular diastolic dysfunction evaluation using KE in Fontan patients [13,14]. At present, the hemodynamic disturbances were neglected in asymptomatic Fontan patients [4]. Our hypothesis was that the consequences of intracardiac flow component and KE parameters might be useful in unraveling the pathophysiological mechanisms of asymptomatic Fontan circulatory dysfunction. The aims of this investigation were to: 1) examine the impact of flow components and kinetic energy (KE) parameters on hemodynamic disturbances in asymptomatic Fontan patients and control group; 2) Assess left ventricular diastolic dysfunction through the analysis of 4D flow parameters across different Fontan sub-groups; 3) Compare intracardiac flow parameters among Fontan sub-groups based on morphological features of the left ventricle (LV) and right ventricle (RV).

2. Materials and methods

2.1. Study population

A retrospective consecutive 25 Fontan patients were enrolled from April 2017 to June 2022. The inclusion criteria were: (1) no previous interventional management such as surgical or catheterization procedures at least in three years after Fontan operation; (2) elder than eight years old patients without sedation who can be cooperative and complete CMR scan; The exclusion criteria:(1) encompassed the presence of other conditions capable of disrupting intra-cardiac flow in pediatric patients. (2) asymptomatic Fontan patients of heart failure, exercise intolerance, abnormalities density of blood, protein losing enteropathy according to clinical diagnosis. (3) Conditions such as pulmonary hypertension, arrhythmia, valvular stenosis, and moderate to severe valvular regurgitation, as well as severe liver, kidney, or lung dysfunction, and inadequate CMR image quality for analysis were observed. We checked patients' blood routine tests in all patients and no more patients were be excluded. The Fontan patients were further categorized into three groups based on their ventricular function: left ventricular (LV), right ventricular (RV), and biventricular (BiV) in Fig. 1. The detailed study design was presented in Fig. 2. Participants for the study were recruited through an online platform. Parents of pediatric volunteers were able to register on the website by providing the necessary

information (https://h.eqxiu.com/s/Mgzk8jcR?eqrcode=1&from=singlemessage&share_level=1&from_user=2022032551a044a1). Pediatric volunteers were selected based on age and gender matching criteria for inclusion in the study. All participants included in the study were pediatric individuals who exhibited normal blood pressure and did not display any signs of cardiovascular disease, as verified through echocardiography. The research methodology was sanctioned by the local research ethics committee, and written consent was acquired from the parent or legal guardian of pediatric volunteers.

2.2. CMR data acquisition and ventricular function analysis

Short-axis cine images of the ventricle, spanning from the base to the apex, were acquired using 2D balanced steady state free precession (2D b-SSFP) cine sequences on a 3.0 T CMR scanner (MR750, GE Healthcare, Milwaukee, WI). Routine 2-, 3- and 4-chamber long-axis and stacks of short-axis cine images were collected with temporal resolution of 30 frames per cardiac cycle. Whole heart 4D flow was performed with free breathing and non-respiratory navigator gating following the SCMR recommendation [8] (Methods in the Data Supplement). The research employed the commercial software CVI 42 Version 5.12.1 (Circle Cardiovascular Imaging, Calgary, Canada) for the post-processing analysis of cardiac magnetic resonance (CMR) images. Cardiac function parameters including end-diastolic volume (EDV), end-systolic volume (ESV), stroke volume (SV), and ventricular mass were obtained from short-axis stacks. Cardiac output (CO) and ejection fraction (EF) were calculated for all participants, with mass and ventricular volumes adjusted for body surface area (BSA). Consistent with prior research, the additional ventricles were excluded from the calculations of ventricular volumes and mass [15].

2.3. Echocardiography image acquisition

The echocardiographic examination was conducted utilizing the Philips CX50 ultrasound machine equipped with a matrix array transducer (S5–1, S8–3) (Philips, Andover, MA, USA). Patients with Fontan physiology underwent echocardiographic imaging in the left lateral decubitus position, with particular attention given to optimizing visualization of mitral inflow. Transthoracic echocardiography was conducted in the apical four-chamber view to capture images, with pulsed wave Doppler utilized to assess trans-mitral early (E) and late (A) diastolic filling velocities, as well as the E/A ratio in Figure S1. Echocardiography was utilized to evaluate left ventricular diastolic dysfunction based on the criteria outlined in the 2016 American Society of Echocardiography guidelines by a single investigator [16].

2.4. Inter-ventricular mechanical dyssynchrony analysis

We semi-automatically tracked left ventricle (LV) lateral wall and right ventricle (RV) free wall deformation in four-chamber long-axis views using our previous published methods of matching by correlation [17]. Time to maximal displacement (T-D_{max}) was determined in both lateral wall and free wall. Inter-ventricular mechanical dyssynchrony was assessed by difference in time to maximal displacement between lateral wall and free wall. Inter-ventricular mechanical dyssynchrony was defined < 0 ms or ≥ 33 ms by 95th percentile from controls (Supplementary Figure S2).

2.5. 4D flow components and kinetic energy

The analysis of Fontan flow data was conducted utilizing the

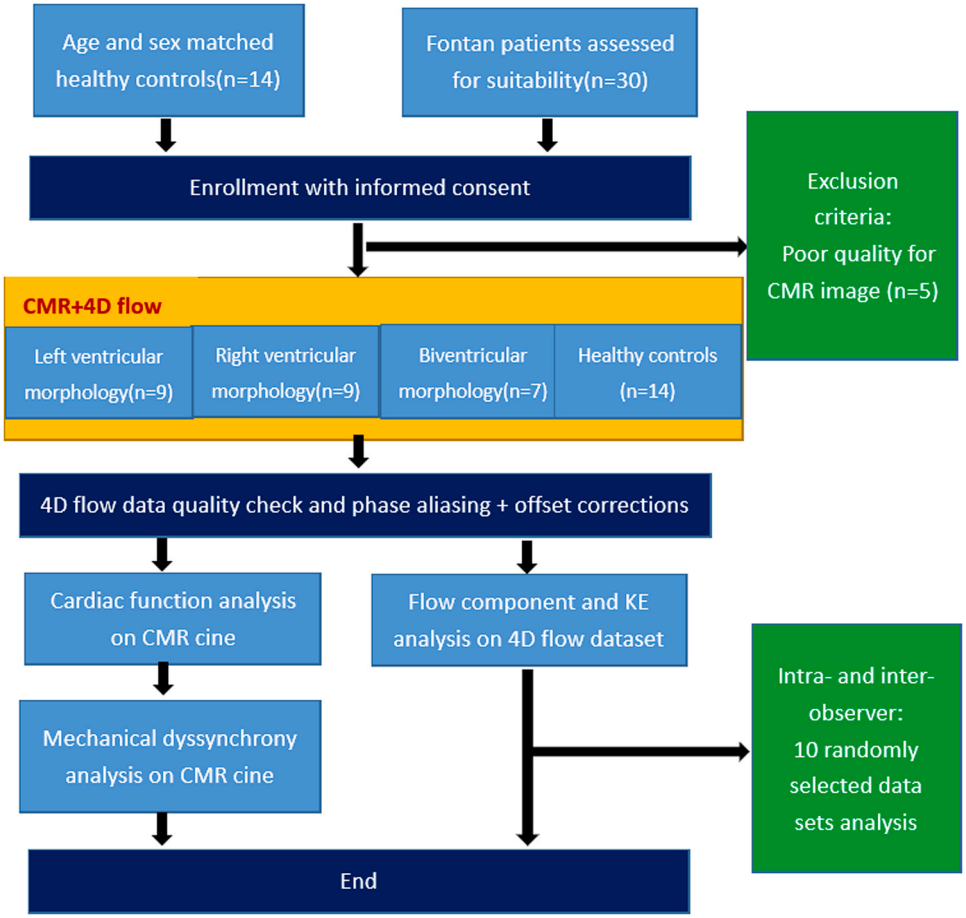

Fig. 2. Study design. 4D = four-dimensional; CMR = cardiovascular magnetic resonance imaging; KE = kinetic energy; CMR =cardiovascular magnetic resonance.

research software MASS (Version 2020EXP) developed by Leiden University Medical Center in Leiden, The Netherlands. The process of automated image-based 3D rigid registration was conducted utilizing the validated Elastix image registration toolbox. [18]. The emitted pathlines at ES were further divided into four functional blood flow components based on their behavior and position. Flow components includes: 1) direct flow; 2) retained inflow; 3) delayed ejection flow; 4) residual volume in Fig. 3. The details of pre-processing analysis were given in the Data Supplement.

For each volumetric element (voxel), the KE was computed using the following formula:$KE = \frac{1}{2}\rho_{blood} \bullet V_{voxel} \bullet v_{voxel}^2$,In this study, the density of blood (1.025 g/cm^3) is denoted as ρ_{blood}, V_{voxel} is the voxel volume and v_{voxel} is the velocity magnitude of the corresponding voxel [12]. The cumulative kinetic energy (KE) within the ventricle was determined in each phase by aggregating the KE values of individual voxels. These KE values were normalized to the ventricular end-diastolic volume (KEi_{EDV}) and then converted to units of microjoules per milliliter (μJ/ml). Time-resolved KE curves were constructed to extract physiologically significant parameters in Fig. 4. 4D flow blood flow and kinetic energy parameters were analyzed in all Fontan subgroups.

2.6. Intra- and inter-observer variability

Intra-observer variability was evaluated by a proficient operator with six years of experience in analyzing 4D CMR, who conducted two blinded assessments of ten randomly selected data sets at intervals exceeding one month. Inter-observer variability was independently assessed by a second observer with twenty years of experience in CMR utilizing the same ten datasets.

2.7. Statistical analysis

All statistical analysis was performed with GraphPad prism version 8.0 (GraphPad, San Diego, USA). All continuous variables were presented as mean ± standard deviation (SD) or median (25th percentile, 75th percentile) as appropriate. Comparisons of Fontan and control groups were conducted with independent *t*-test analysis for normally distributed data and Mann-Whitney test for non-normally distributed continuous variable. The demographic and clinical characteristics of three groups were evaluated using unpaired one-way analysis of variance (ANOVA) for normally distributed variables, the Kruskal-Wallis test for non-normally distributed variables, and Fisher's exact test for categorical variables. Receiver operator characteristic (ROC) analysis was employed to evaluate the predictive capacity of 4D flow parameters for diastolic dysfunction. Intra- and inter-observer reproducibility were determined through intraclass correlation coefficient (ICC) and coefficient of variation (COV). Statistical significance was defined as a *P* value less than 0.05.

3. Results

3.1. Participant characteristics and ventricular function

Of the total 25 Fontan patients (M/F: 15/10), 9 (M/F: 6/3) had a functional single ventricle (left ventricle type) (6 tricuspid atresia, 3 pulmonary atresia with intact ventricular septum), 9 (M/F: 4/5) had functional single ventricle (right ventricle type) (2 single right ventricle, 5 double outlet of right ventricle, 1 complete transposition of the great arteries, 1 total anomalous pulmonary venous connection), and 7 (M/F: 5/2) had functional single ventricle (biventricular type); 25 had an extracardiac conduit **(**Table 1**)**. New York Heart Association functional class I–II was seen in all patients (100 %). The interquartile range (IQR) postoperative follow-up time of CMR was 5 (3,7) years. 9 cases had LV diastolic dysfunction from echocardiography in 16 Fontan patients (single RVs were excluded from these analyses). There were no significant differences between Fontan patients and control groups for mass index ($P = 0.588$), EDV index ($P = 0.671$), ESV index ($P = 0.151$), SV index ($P = 0.580$), EF ($P = 0.142$), and cardiac index ($P = 0.271$) **(**Table 2**)**. Fontan patients exhibited significantly greater inter-ventricular mechanical synchrony indexes compared to healthy controls, with the time to maximal displacement consistently longer in the right ventricular free wall than the left ventricular lateral wall (-11 [-60, 32] ms vs. 11 [0,25] ms, $P < 0.05$) **(**Supplementary Figure S2**)**.

3.2. Changes in 4D flow components, kinetic energy and inter-ventricular mechanical dyssynchrony profiles

The median direct flow (32 % vs. 40 %) and delayed ejection flow (17 % vs. 24 %) were found to be significantly lower, while residual volume (28 % vs. 23 %) was significantly higher in Fontan patients when compared to a normal control group (all $P < 0.05$, Table 2). There was no significant differences in retained inflow between two groups (18 % vs. 12 %, $P = 0.072$).

There were significant differences in all KE parameters in Fontan patients compared to normal controls **(**Table 2**)**. There were significant decreases in regional (basal, mid and apical) kinetic energy parameters in Fontan patients (all $P < 0.001$), except for basal peak A-wave KE_{iEDV} ($P = 0.100$) (Table 3). Peak systolic and E-wave KEi_{EDV} with different EF were decreased compared to normal control ($P < 0.001$) (Fig. 5).

The inter-ventricular dyssynchrony included LV subtype (5 cases), RV subtype (6 cases), and biventricular subtype (4 cases) in Fontan group. There were no statistically significant differences observed in flow components and kinetic energy parameters between Fontan patients with inter-ventricular mechanical dyssynchrony and those without inter-ventricular dyssynchrony. **(**Table 4**)**.

3.3. Association of 4D flow parameters with LV diastolic dysfunction

No significant difference was observed for 4D flow parameters between Fontan patients with and without LV diastolic dysfunction group (single RVs were excluded from these analyses), except for median direct flow (38 % vs. 30 %, $P = 0.031$) (Table 5). ROC analysis demonstrated that direct flow (AUC = 0.760) had better discrimination for LV diastolic dysfunction than retained inflow (AUC = 0.533), delayed ejection flow (AUC = 0.567), residual volume (AUC = 0.653) and EF (AUC = 0.50) (Fig. 6 **and** Supplementary Table S1).

3.4. Disruption of intracardiac flow in fontan groups with morphologic LV or RV

There were no significant differences in 4D flow components between patients with morphologic left ventricle and those with morphologic right ventricle, except for median residual volume. (24 % vs. 33 %, $P = 0.020$). There were no significant difference in KE parameters except morphologic RV subgroup having lower median peak E-wave KEi_{EDV} than morphologic LV subgroup (11.2 vs. 12.4 μJ/ml, $P = 0.002$) (Supplementary Table S2).

3.5. Intra and inter-observer variability

Intra-observer agreement was good for the 4D flow components and KE parameters (ICC = 85.3 % - 99.6 %, COV = 1.62 % - 6.58 %). Inter-observer agreement was good (ICC = 82.1 % - 98.1 %, COV = 3.29 % −11.24 %) (Supplementary Table S3).

4. Discussion

In this study, we conducted a retrospective, single-center investigation to evaluate the flow components and KE parameters, as well as examine the disturbance of intracardiac flow patterns in patients with single ventricle physiology. Our primary findings are as follows: (1)

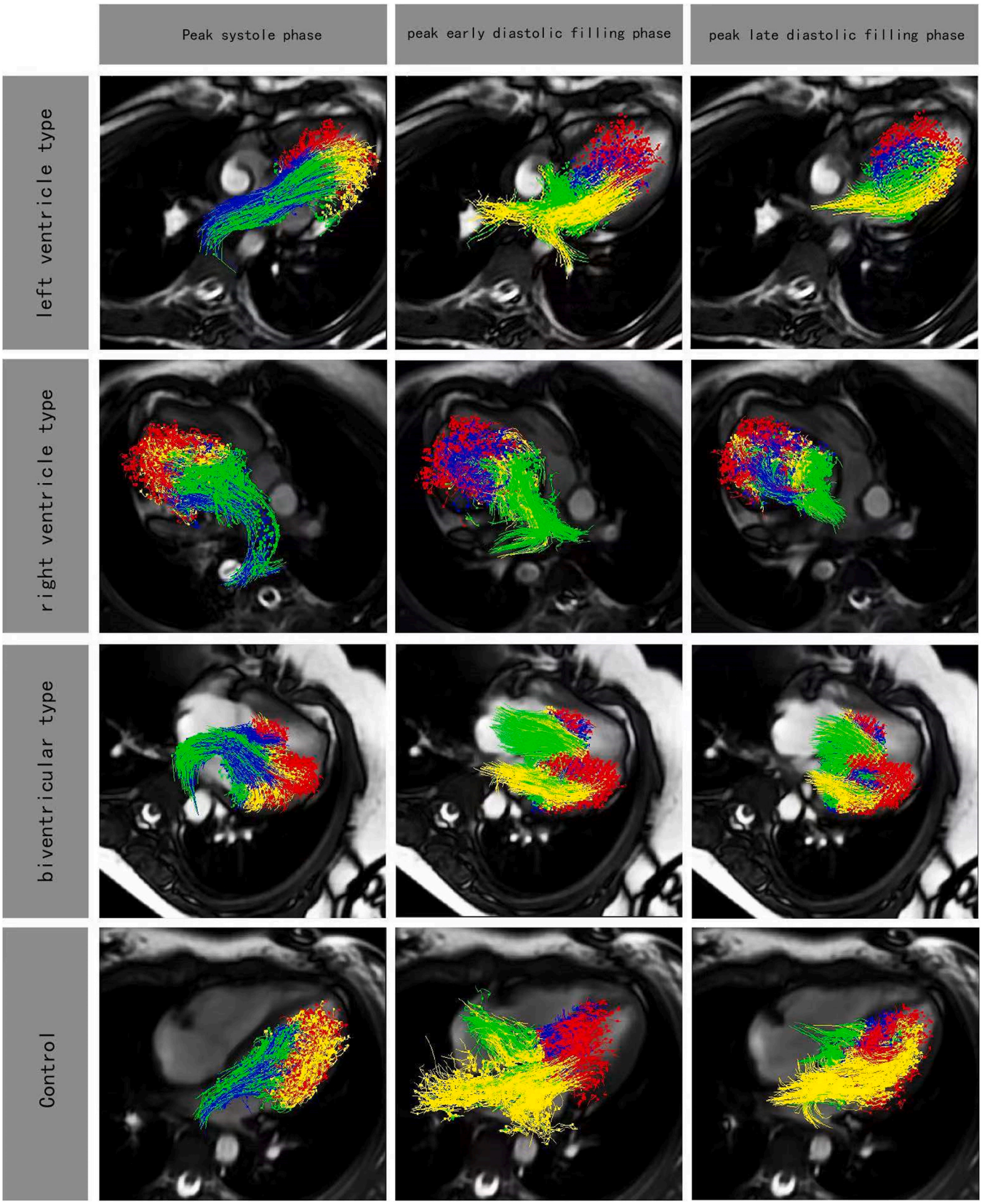

Fig. 3. Four-chamber views with particle tracing superimposed at peak systole, peak early diastolic filling, and peak late diastolic filling phases in Fontan patients. (LV type, RV type, biventricular type) and control. Red, blue, yellow and green color represented residual volume, delayed ejection flow, retained inflow and direct flow, respectively.

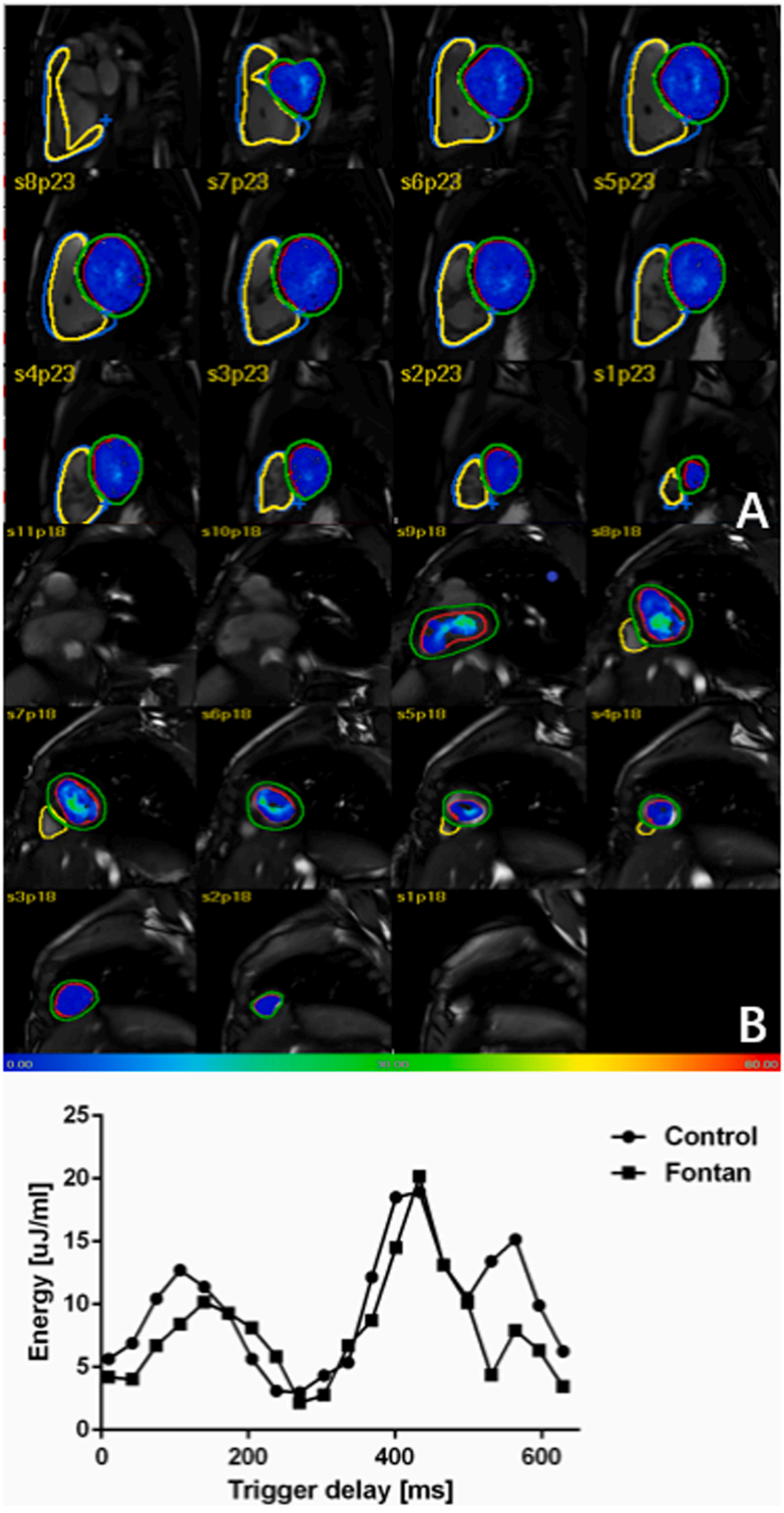

Fig. 4. KE evaluation within one heart beat cycle. (A). KE color maps on short axis view in normal control; (B). KE color maps on short axis view in Fontan patient.

Table 1
Characteristics of the Fontan patients.

Diagnosis	n	Type of Fontan
Left ventricular morphology	9	
Tricuspid atresia	6	Extracardiac
Pulmonary atresia	3	Extracardiac
Right ventricular morphology	9	
Double outlet right ventricle, ventricular septal defect	5	Extracardiac
Single right ventricle	2	Extracardiac
Total anomalous pulmonary venous connection, ventricular septal defect	1	Extracardiac
Complete transposition of the great arteries, ventricular septal defect	1	Extracardiac
Biventricular morphology	7	
Double outlet right ventricle	3	Extracardiac
Pulmonary stenosis	1	Extracardiac
Transposition of the Great Arteries, ventricular septal defect	2	Extracardiac
Pulmonary atresia	1	Extracardiac

Table 2
Demographics and 4D flow parameters in Fontan patients and control.

Parameters	Control (n = 14)	Fontan (n = 25)	*P*
Demographics			
Age, years	10 (9, 11)	9 (8, 12)	0.836
Follow-up time since surgery, years	-	5 (3, 7)	-
Gender, M/F	8/6 (57 %)	15/10 (60 %)	0.866
Height, cm	144 (132, 150)	125 (120, 135)	**0.039**
Weight, kg	37 (28, 45)	25 (20, 31)	**0.008**
Body surface area, m^2	1.22 (1.02,1.37)	0.93 (0.82, 1.05)	**0.012**
Systolic blood pressure, mmHg	114 (109,118)	112 (107,116)	0.624
Diastolic blood pressure, mmHg	69 (65,73)	66 (61,71)	0.228
Heart rate, bpm	77 (71, 87)	79 (62, 93)	0.745
NYHA functional class I–II		25(100 %)	-
Mass index, g/m^2	38 (35, 40)	37 (29, 46)	0.588
EDV index, ml/m^2	73 (64, 86)	80 (57, 100)	0.671
ESV index, ml/m^2	31 (29, 35)	38 (27, 44)	0.151
SV index, ml/m^2	39 (35, 52)	41 (30, 57)	0.580
Ejection fraction, %	58 (56, 60)	56 (51, 63)	0.142
Cardiac output, L/min	3.64 (3.21, 4.14)	3.21 (2.65, 3.72)	0.298
Cardiac output index, $L/min/m^2$	4.05 (3.32, 4.76)	3.39 (2.19, 4.27)	0.271
E-wave velocities, cm/s	-	79.68 (56.7,96.5)	-
A-wave velocities, cm/s	-	58.28(43.2,76)	-
E/A ratio	-	1.54(1,2.05)	-
LV Diastolic dysfunction, n	0 (%)	9/16 * (56 %)	-
Blood flow components			
Direct flow, %	40 (37, 41)	32 (28, 39)	**0.005**
Retained inflow, %	12 (10, 16)	18 (12, 24)	0.072
Delayed ejection flow, %	24 (19, 27)	17 (13, 23)	**0.024**
Residual volume, %	23 (18, 29)	28 (24, 35)	**0.034**
KE indexed to EDV			
Average KEi_{EDV}, μJ/ml	11.2 (9.8, 14.3)	6.6 (4.6, 8.1)	**< 0.001**
Peak systolic KEi_{EDV}, μJ/ml	23.5 (20.7, 27.5)	11.7 (9.4, 16.3)	**< 0.001**
Systolic KEi_{EDV}, μJ/ml	11.7 (9.6, 15.6)	6.7 (4.7, 8.4)	**< 0.001**
Diastolic KEi_{EDV}, μJ/ml	11.8 (8.6, 14.5)	6.5 (4.3, 8.6)	**< 0.001**
Peak E-wave KEi_{EDV}, μJ/ml	27.5 (23.6, 31.7)	11.7 (9.1, 15.3)	**< 0.001**
Peak A-wave KEi_{EDV}, μJ/ml	12.1 (9.8, 13.7)	8.3 (4.8, 10.9)	**0.019**
KEi_{EDV} E/A ratio	2.38 (1.92, 2.71)	1.44 (1.07, 2.48)	**0.02**

Data are reported as median (25th percentile, 75th percentile). There were statistical differences in bold representation. NYHA = New York Heart Association functional class; EDV = end-diastolic volume; ESV = end-systolic volume; SV = stroke volume; LV = left ventricle; KE = Kinetic energy; KE_{iEDV} = KE index ventricular end-diastolic volume. * : 9 Fontan (right ventricle type) not included.

Direct flow and residual volume may serve as indicators for assessing between Fontan patients and controls; (2) all KE parameters exhibited a decrease in Fontan patients; (3) direct flow proved to be the most effective flow component marker for predicting LV diastolic dysfunction

Table 3
Comparison of regional kinetic energy (KE) parameters between Fontan patients and volunteers.

Parameters	Control (n = 14)	Fontan (n = 25)	*P*
Basal KE indexed to EDV			
Average KEi_{EDV}, μJ/ml	7.5 (6.5, 8.9)	4.3 (3.3, 5.4)	< 0.001
Peak systolic KEi_{EDV}, μJ/ml	16.0 (12.5, 18.0)	9.4 (6.6, 10.9)	< 0.001
Systolic KEi_{EDV}, μJ/ml	8.9 (6.1, 8.9)	4.2 (3.5, 5.4)	< 0.001
Diastolic KEi_{EDV}, μJ/ml	7.2 (6.3, 8.8)	3.6 (2.5, 5.3)	< 0.001
Peak E-wave KEi_{EDV}, μJ/ml	18.5 (15.9, 20.3)	8.0 (6.1, 10.3)	< 0.001
Peak A-wave KEi_{EDV}, μJ/ml	7.2 (5.6, 7.8)	4.7 (2.9, 7.3)	0.100
KEi_{EDV} E/A ratio	2.72 (1.94, 3.45)	1.70 (1.13, 2.57)	0.006
Mid KE indexed to EDV			
Average KEi_{EDV}, μJ/ml	3.3 (2.9, 4.0)	1.6 (1.2, 2.4)	< 0.001
Peak systolic KEi_{EDV}, μJ/ml	4.8 (3.8, 5.7)	2.8 (1.8, 3.6)	< 0.001
Systolic KEi_{EDV}, μJ/ml	2.7 (2.5, 3.3)	1.7 (1.1, 2.1)	0.001
Diastolic KEi_{EDV}, μJ/ml	4.1 (3.2, 4.7)	1.7 (1.3, 2.7)	< 0.001
Peak E-wave KEi_{EDV}, μJ/ml	8.3 (6.6, 11.2)	3.2 (2.3, 4.2)	< 0.001
Peak A-wave KEi_{EDV}, μJ/ml	3.9 (3.2, 5.1)	2.4 (1.4, 3.1)	0.002
KEi_{EDV} E/A ratio	2.11 (1.57, 3.12)	1.28 (1.03, 2.33)	0.021
Apical KE indexed to EDV			
Average KEi_{EDV}, μJ/ml	0.8 (0.6, 1.3)	0.2 (0.2, 0.4)	< 0.001
Peak systolic KEi_{EDV}, μJ/ml	1.5 (1.3, 1.9)	0.5 (0.3, 0.7)	< 0.001
Systolic KEi_{EDV}, μJ/ml	0.8 (0.7, 1.0)	0.3 (0.2, 0.4)	< 0.001
Diastolic KEi_{EDV}, μJ/ml	0.7 (0.6, 1.3)	0.3 (0.1, 0.4)	< 0.001
Peak E-wave KEi_{EDV}, μJ/ml	1.3 (0.8, 1.9)	0.4 (0.2, 0.7)	< 0.001
Peak A-wave KEi_{EDV}, μJ/ml	1.3 (1.0, 1.9)	0.3 (0.2, 0.5)	< 0.001
KEi_{EDV} E/A ratio	0.84 (0.63, 1.23)	1.16 (0.87, 2.05)	0.037

Data are reported as median (25th percentile, 75th percentile). There were statistical differences in bold representation; EDV = end-diastolic volume.

in both LV and BiV Fontan subgroups; (4) the LV Fontan subgroup demonstrated a more efficient intracardiac flow pattern.

4.1. The characteristics of intracardiac flow components

Previous research has demonstrated that individuals with seemingly compensated dilated cardiomyopathy (DCM) exhibit altered patterns of left ventricular (LV) flow [19]. It is commonly acknowledged that direct flow follows an optimal pathway to the ventricular outflow tract, adhering to the shortest distance. Conversely, the residual volume is located at the periphery of the ventricular cavity and serves to demarcate the functional boundary of the chamber [20]. In our study, we observed a significant difference between the Fontan group and the control group in terms of decreased median direct flow (32 % vs. 40 %, $P = 0.005$) and increased median residual volume (28 % vs. 23 %, $P < 0.05$). These findings indicate a highly inefficient flow pattern. Highly inefficient flow pattern was measured according to intraventricular flow partitioning by 4D Flow CMR [21]. The reason might be that the lower cardiac efficiency was interchanged predominantly from the delayed ejection flow and the retained inflow to residual volume, we figured that was the results of energy transferring from the inflow components. Our findings were consistent with those of Stone et al. [22].

On the contrary, Bolger et al. [23] have shown that the inflow retained in a typical left ventricle must decelerate at the conclusion of diastole and then accumulate further kinetic energy before being ejected during the subsequent systole. In our study, we observed a significant difference in the median delayed ejection flow between the Fontan's group and the control group (17 % vs. 24 %, $P < 0.05$). This finding may provide insight into the compensatory mechanisms in post-Fontan patients through intracardiac flow components.

4.2. The function of KE in fontan patients

The assessment of kinetic energy serves as a measure of the heart's efficiency in expelling blood. Sjöberg Pia et al. [12] documented the maximum diastolic kinetic energy in Fontan patients, while Kamphuis et al. [24] found that elastic load was notably higher in Fontan patients compared to the control group. In our study, KE parameters of Fontan

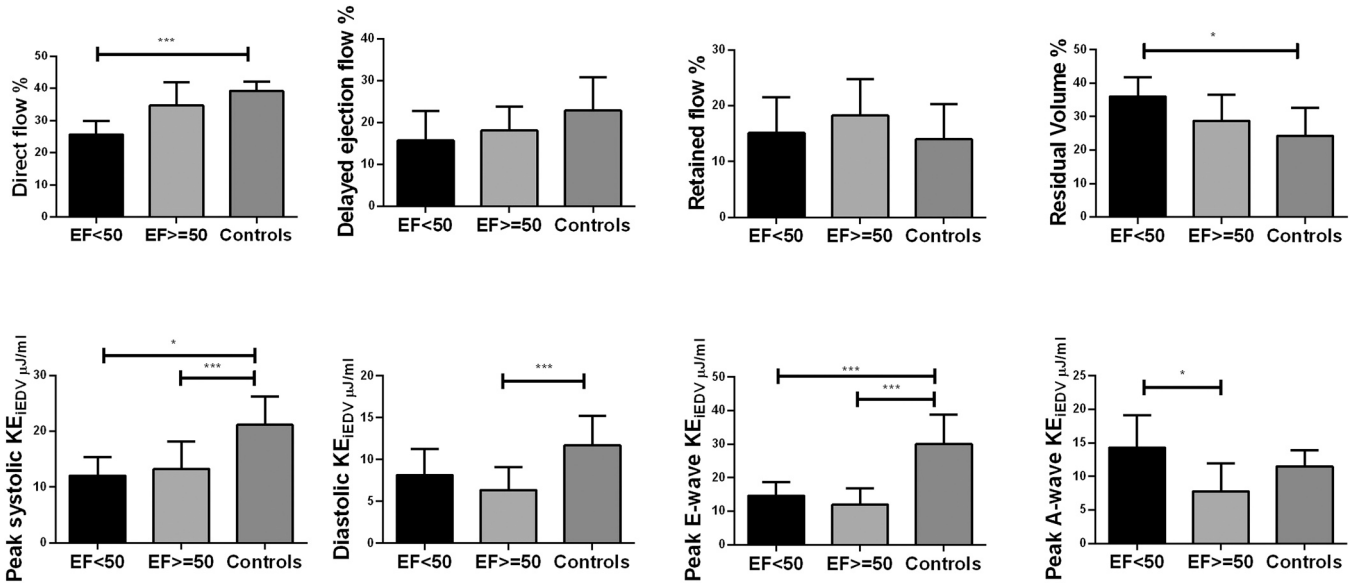

Fig. 5. Differences in ventricular flow components which included peak systolic kinetic energy indexed (peak systolic KEi_{EDV}), indexed average diastolic KEi_{EDV}, indexed peak E-wave KEi_{EDV} and indexed peak A-wave KEi_{EDV} according to different ejection fraction. EF: ≥ =50 % (n = 20); < 50 % (n = 5); Controls≥ 55 % (n = 14). KEi_{EDV} = kinetic energy normalized to end-diastolic volume. Bars showed mean value, and error bars indicated SD. *$P < 0.05$ compared with healthy controls; * **$P < 0.001$ compared with healthy controls.

Table 4
Comparison of 4D flow parameters between Fontan patients with inter-ventricular mechanical dyssynchrony versus without inter-ventricular dyssynchrony.

4D flow parameters	Fontan with inter-ventricular mechanical dyssynchrony (n = 15)*	Fontan without inter-ventricular mechanical dyssynchrony (n = 9)	*P*
Blood flow components			
Direct flow, %	34 (29, 39)	29 (25, 37)	0.272
Retained inflow, %	18 (17, 21)	12 (8, 25)	0.814
Delayed ejection flow, %	17 (12, 23)	17 (14, 23)	0.859
Residual volume, %	27 (24, 32)	33 (27, 40)	0.162
KE indexed to EDV			
Average KEi_{EDV}, µJ/ml	7.0 (5.0,9.7)	6.3 (4.4, 8.1)	0.682
Peak systolic KEi_{EDV}, µJ/ml	11.3 (9.9, 15.1)	13.4 (10.4, 19.4)	0.347
Systolic KEi_{EDV}, µJ/ml	6.7 (5.2, 7.5)	7.1 (4.7, 9.7)	0.861
Diastolic KEi_{EDV}, µJ/ml	7.8 (4.6, 9.3)	5.3 (4.0, 6.8)	0.181
Peak E-wave KEi_{EDV}, µJ/ml	14.0 (9.2, 16.7)	11.2 (9.0, 12.1)	0.131
Peak A-wave KEi_{EDV}, µJ/ml	9.8 (4.6, 13.9)	7.3 (5.7, 10.7)	0.432
KEi_{EDV} E/A ratio	1.44 (1.01, 2.66)	1.38 (1.11, 2.06)	0.788

Data were reported as median (25th percentile, 75th percentile). KEi_{EDV} = kinetic energy normalized to end-diastolic volume (EDV). Inter-ventricular dyssynchrony assessed by difference in time to maximal displacement between RV free wall and LV lateral wall (i.e. ≥33 ms by 95th percentile from controls). *One case was excluded due to poor image quality.

Table 5
Comparison of 4D flow blood flow and kinetic energy parameters between Fontan patients with and without left ventricular diastolic dysfunction.

Parameters	Fontan with diastolic dysfunction (n = 9)	Fontan without diastolic dysfunction (n = 7)	*P*
Blood flow components			
Direct flow, %	30 (26, 34)	38 (31, 42)	0.031
Retained inflow, %	19 (12, 24)	17 (12, 22)	0.807
Delayed ejection flow, %	17 (13, 23)	17 (12, 21)	0.605
Residual volume, %	29 (25, 40)	26 (24, 31)	0.216
KE indexed to EDV			
Average KEi_{EDV}, µJ/ml	6.6 (4.8, 8.8)	6.2 (3.8, 7.7)	0.428
Peak systolic KEi_{EDV}, µJ/ml	13.1 (10.0, 17.1)	10.9 (8.5, 13.3)	0.160
Systolic KEi_{EDV}, µJ/ml	7.1 (5.4, 10.0)	5.8 (3.8, 7.5)	0.144
Diastolic KEi_{EDV}, µJ/ml	6.3 (4.6, 9.3)	7.1 (3.7, 8.6)	0.978
Peak E-wave KEi_{EDV}, µJ/ml	11.2 (9.1, 15.2)	11.9 (8.6, 15.8)	0.892
Peak A-wave KEi_{EDV}, µJ/ml	8.1 (5.2, 10.3)	10.1 (2.5, 12.2)	0.935
KEi_{EDV} E/A ratio	1.49 (1.01, 2.03)	1.44 (1.08, 2.91)	0.683

Data were reported as median (25th percentile, 75th percentile). There were statistical differences in bold representation. EDV = end-diastolic volume. KEi_{EDV} = kinetic energy normalized to end-diastolic volume.

patients were lower than these of controls. Peak systolic and diastolic KEi_{EDV} of patients were significantly lower than these of controls in regional parameters (age 10 ± 3 years). David and his colleagues [14] reported peak systolic KE were significantly higher in Fontan patients than in healthy volunteers (age 26 ± 8 years). Our explanation was that impaired myocardial systolic function resulted in inefficient kinetic energy for pediatric Fontan patients. Alterations in ventricular KE may serve as an indicator of ventricular dysfunction [25]. We found that peak A-wave KEi_{EDV} was not significantly different in the ventricular base (5µJ/ml vs. 7µJ/ml, $P > 0.05$). We understood that compensatory mechanism of atrial booster had not been launched in early Fontan patients [26]. Utilizing kinetic energy as a metric for assessing effective cardiac function may enhance our comprehension of compromised ventricular filling efficacy.

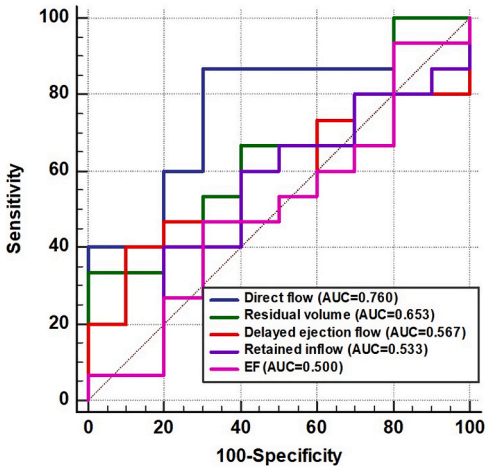

Fig. 6. 4D Flow component and ejection fraction assess impaired LV diastolic function. Diastolic function (n = 9) versus diastolic dysfunction (n = 7) in 16 Fontan patients (single RVs were excluded from these analyses). KE = kinetic energy; EF = ejection fraction; LV = left ventricle;RV = right ventricle.

4.3. Assessment of diastolic dysfunction in fontan group

Our research findings indicate that direct flow is a more reliable indicator of diastolic dysfunction compared to other intracardiac flow components and kinetic energy parameters. Stoll et al. [18] found that the average kinetic energy of direct flow was a significant predictor of functional capacity in individuals with heart failure. Zhao et al. [27] proved that direct flow was independent predictors of right ventricle remodeling index in repaired Tetralogy of Fallot patients. Direct flow was an important marker that were best confirmed with longitudinal assessment.

Previous research conducted on both children and adults with Fontan FSV had indicated a notable prevalence of ventricular dyssynchrony [28–31]. Rösner et al. [32] had demonstrated a correlation between ventricular dyssynchrony in the Fontan circulation and impaired systolic and diastolic function. Within our subgroup of 24 Fontan patients (One case was excluded due to poor image quality), fifteen individuals demonstrated ventricular dyssynchrony (included LV subtype 5 cases, RV subtype 6 cases, and biventricular subtype 4 cases), indicating an increased vulnerability of the univentricular heart to myocardial dysfunction when intraventricular conduction delay is present. However, our study findings indicate that inter-ventricular dyssynchrony does not yield any statistically significant differences on flow components and KE parameters in Fontan patients.

4.4. Intracardiac flow in single ventricle physiology

The anomalous intracardiac anatomy present in Fontan patients resulted in alterations in intraventricular flow patterns, which may be investigated and assessed through the analysis of flow component and kinetic energy parameters. By comparing subgroups of LV and RV, we discovered an increase in residual flow and a decrease in peak E-wave KE_{iEDV} in the RV Fontan subgroup. These differences suggested that the LV subgroup exhibited a more efficient intracardiac flow pattern in patients with Fontan circulation. This finding aligns with previous research [14]. Conversely, in the RV subgroup, characterized by fused inflow and a highly spherical ventricle (Figure S3). A vortex ring was generated and its advancement towards the apex was hindered by circumferential propagation, resulting in reduced filling velocities and dissipation of kinetic energy [24].

4.5. Limitations

This study is subject to certain limitations that merit consideration. Firstly, the sample size of this retrospective study was relatively small, and heterogeneity within the group remains. Secondly, while previous research has shown that non-respiratory navigated acquisition of 4D flow yielded comparable results to respiratory navigated acquisition in terms of image quality assessment [33], 5 cases still had poor CMR images without non-respiratory navigator gating in our study. Thirdly, T1 mapping and extracellular volume were not included in our study, it might provide a better understanding of the pathogenesis of progressive functional single ventricular. Fourthly, it is possible that changes in heart rate may lead to alterations in the proportions of flow components to accommodate the extended diastolic period, while ensuring the effectiveness of the systolic ejection phase is maintained. Fifthly, none of pediatric Fontan patients underwent cardiopulmonary exercise testing (CPET) due to logistical reasons. Sixthly, evaluation diastolic function by correlation echocardiogram and invasive catheterization measurements would be more helpful. Unfortunately, the assessment of catheter diastolic function was not included in our study. Seventhly, the study assessed asymptomatic individuals with Fontan circulation as well as control subjects. Cases of heart failure in Fontan patients were excluded from the analysis. The potential future implications of utilizing 4D flow CMR imaging parameters in Fontan patients may lead to a redefinition of risk prognostication and could potentially inform treatment decision-making processes.

5. Conclusions

The altered flow pattern and reduced kinetic energy observed in Fontan patients may indicate hemodynamic disturbances and compromised ventricular filling. Reduced direct flow is associated with LV diastolic dysfunction in LV and BiV Fontan subgroups. Systemic LV exhibited a more efficient intracardiac flow pattern compare with systemic RV in Fontan patients.

Disclosure

All authors have read and approved the final manuscript and have no conflicts of interest to declare.

Funding

This study was supported by grants from the National Key Clinical Specialties Construction Program, Innovative research team of high-level local universities in Shanghai, National Natural Science Foundation of China (No. 82171902), the Shanghai Committee of Science and Technology (No. 17411965400, 22TS1400800) and SJTU Trans-med Awards Research (No. 20220101).

CRediT authorship contribution statement

Liang Zhong: Writing – review & editing. **Yu-Min Zhong:** Writing – review & editing, Funding acquisition, Conceptualization. **Li-Wei Hu:** Writing – original draft, Formal analysis, Data curation. **Ai-Min Sun:** Data curation. **Yi-Man Liu:** Data curation. **Wei Dong:** Data curation. **Xiaodan Zhao:** Writing – original draft, Formal analysis, Data curation. **Shuang Leng:** Methodology. **RongZhen Ouyang:** Visualization, Investigation. **Qian Wang:** Investigation.

Declaration of Competing Interest

The authors declare that they have no known competing financial interests or personal relationships that could have appeared to influence the work reported in this paper.

Acknowledgements

Not applicable.

Ethics approval and consent to participate

Not applicable.

Consent for publication

Not applicable.

Informed Consent Statement

Our registry was generated in de-identified form, so the requirement for written informed consent was waived.

Appendix A. Supporting information

Supplementary data associated with this article can be found in the online version at doi:10.1016/j.ejro.2024.100631.

Data Availability

The datasets utilized during the present study can be obtained from the corresponding author upon a reasonable request.

References

[1] S.Y. Tseng, S. Siddiqui, M.V. Di Maria, et al., Atrioventricular valve regurgitation in single ventricle heart disease: a common problem associated with progressive deterioration and mortality, J. Am. Heart Assoc. 9 (2020) e015737, https://doi.org/10.1161/JAHA.119.015737.
[2] A. Kato, E. Riesenkampff, D. Yim, et al., Pediatric Fontan patients are at risk for myocardial fibrotic remodeling and dysfunction, Int J. Cardiol. 240 (2017) 172–177, https://doi.org/10.1016/j.ijcard.2017.04.073.
[3] J. Logoteta, C. Ruppel, J.H. Hansen, et al., Ventricular function and ventriculo-arterial coupling after palliation of hypoplastic left heart syndrome: A comparative study with Fontan patients with LV morphology, Int J. Cardiol. 227 (2017) 691–697, https://doi.org/10.1016/j.ijcard.2016.10.076.
[4] W. Budts, W.J. Ravekes, D.A. Danford, S. Kutty, Diastolic Heart failure in patients with the Fontan circulation: a review, JAMA Cardiol. 5 (2020) 590–597, https://doi.org/10.1001/jamacardio.2019.5459.
[5] W.R. Miranda, B.A. Borlaug, C.C. Jain, et al., Exercise-induced changes in pulmonary artery wedge pressure in adults post-Fontan versus heart failure with preserved ejection fraction and non-cardiac dyspnoea, Eur. J. Heart Fail 25 (1) (2023) 17–25, https://doi.org/10.1002/ejhf.2706.
[6] A.N. Gupta, M. Markl, M.S.M. Elbaz, Intracardiac and vascular hemodynamics with cardiovascular magnetic resonance in heart failure.[J], Heart Fail Clin. 17 (2021) 135–147, https://doi.org/10.1016/j.hfc.2020.08.010.
[7] G. Soulat, P. McCarthy, M. Markl, 4D flow with MRI, Annu Rev. Biomed. Eng. 22 (2020) 103–126, https://doi.org/10.1146/annurev-bioeng-100219-110055.
[8] J. Garcia, A.J. Barker, M. Markl, The role of imaging of flow patterns by 4D flow MRI in aortic stenosis, JACC Cardiovasc Imaging 12 (2019) 252–266, https://doi.org/10.1016/j.jcmg.2018.10.034.
[9] Petter Dyverfeldt, Malenka Bissell, Alex J. Barker, et al., 4D flow cardiovascular magnetic resonance consensus statement, J. Cardiovasc Magn. Reson 17 (2015) 72, https://doi.org/10.1186/s12968-023-00942-z.
[10] L. Zhong, E.M. Schrauben, J. Garcia, et al., Intracardiac 4D Flow MRI in congenital heart disease: recommendations on behalf of the ISMRM flow & motion study group: intracardiac 4D flow MRI in CHD, J. Magn. Reson Imaging 50 (2019) 677–681, https://doi.org/10.1002/jmri.26893.
[11] J. Wong, R. Chabiniok, S.M. Tibby, et al., Exploring kinetic energy as a new marker of cardiac function in the single ventricle circulation, J. Appl. Physiol. 125 (2018) 889–900, https://doi.org/10.1152/japplphysiol.00580.2017.
[12] V.P. Kamphuis, M.S.M. Elbaz, P.J. van den Boogaard, et al., Stress increases intracardiac 4D flow cardiovascular magnetic resonance -derived energetics and vorticity and relates to VO2max in Fontan patients, J. Cardiovasc Magn. Reson 21 (2019) 43, https://doi.org/10.1186/s12968-019-0553-4.
[13] P. Sjöberg, E. Heiberg, P. Wingren, et al., Decreased diastolic ventricular kinetic energy in young patients with Fontan circulation demonstrated by four-dimensional cardiac magnetic resonance imaging, Pedia Cardiol. 38 (2017) 669–680, https://doi.org/10.1007/s00246-016-1565-6.
[14] D.R. Rutkowski, G. Barton, C.J. François, H.L. Bartlett, et al., Analysis of cavopulmonary and cardiac flow characteristics in fontan patients: comparison with healthy volunteers, J. Magn. Reson Imaging 49 (2019) 1786–1799, https://doi.org/10.1002/jmri.26583.
[15] Liwei Hu, Aimin Sun, Chen Guo, et al., Assessment of global and regional strain left ventricular in patients with preserved ejection fraction after Fontan operation using a tissue tracking technique, Int J. Cardiovasc Imaging 35 (2019) 153–160, https://doi.org/10.1007/s10554-018-1440-z.
[16] S.F. Nagueh, O.A. Smiseth, C.P. Appleton, et al., Recommendations for the evaluation of left ventricular diastolic function by echocardiography: an update from the American society of echocardiography and the European association of cardiovascular imaging, J. Am. Soc. Echocardiogr. 29 (2016) 277–314, https://doi.org/10.1093/ehjci/jew082.
[17] S. Leng, X.D. Zhao, F.Q. Huang, et al., Automated quantitative assessment of cardiovascular magnetic resonance-derived atrioventricular junction velocities, Am. J. Physiol. Heart Circ. Physiol. 309 (2015) 1923–1935, https://doi.org/10.1152/ajpheart.00284.2015.
[18] S. Klein, M. Staring, K. Murphy, et al., elastix: a toolbox for intensity-based medical image registration.[J], IEEE Trans. Med Imaging 29 (2010) 196–205, https://doi.org/10.1109/TMI.2009.2035616.
[19] Stoll V.M., Hess A.T., Rodgers C.T. et al. Left ventricular flow analysis. Circ Cardiovasc Imaging.2019, 12,e008130. Doi:10.1161/CIRCIMAGING.118.008130.
[20] J. Eriksson, A.F. Bolger, T. Ebbers, et al., Four-dimensional blood flow-specific markers of LV dysfunction in dilated cardiomyopathy, Eur. Heart J. Cardiovasc Imaging 14 (2013) 417–424, https://doi.org/10.1093/ehjci/jes159.
[21] J. Eriksson, P. Dyverfeldt, J. Engvall, et al., Quantification of presystolic blood flow organization and energetics in the human left ventricle, Am. J. Physiol. Heart Circ. Physiol. 300 (2011) 2135–2141, https://doi.org/10.1152/ajpheart.00993.2010.
[22] M.L. Stone, M. Schäfer, M.V. DiMaria, et al., Diastolic inflow is associated with inefficient ventricular flow dynamics in Fontan patients, J. Thorac. Cardiovasc Surg. 163 (2022) 1195–1207, https://doi.org/10.1016/j.jtcvs.2021.06.064.
[23] A.F. Bolger, E. Heiberg, M. Karlsson, et al., Transit of blood flow through the human left ventricle mapped by cardiovascular magnetic resonance, J. Cardiovasc Magn. Reson 9 (2007) 741–747, https://doi.org/10.1080/10976640701544530.
[24] V.P. Kamphuis, M.S.M. Elbaz, P.J. van den Boogaard, et al., Disproportionate intraventricular viscous energy loss in Fontan patients: analysis by 4D flow MRI, Eur. Heart J. Cardiovasc Imaging 20 (2013) 323–333, https://doi.org/10.1093/ehjci/jey096.
[25] D. Jeong, P.V. Anagnostopoulos, A. Roldan-Alzate, et al., Ventricular kinetic energy may provide a novel noninvasive way to assess ventricular performance in patients with repaired tetralogy of Fallot, J. Thorac. Cardiovasc Surg. 149 (5) (2015) 1339–1347, https://doi.org/10.1016/j.jtcvs.2014.11.085.
[26] D. Aronson, H. Sliman, S. Abadi, et al., Conduit flow compensates for impaired left atrial passive and booster functions in advanced diastolic dysfunction, Circ. Cardiovasc Imaging 17 (5) (2024) e016276, https://doi.org/10.1161/CIRCIMAGING.123.016276.
[27] X. Zhao, L. Hu, S. Leng, et al., Ventricular flow analysis and its association with exertional capacity in repaired tetralogy of Fallot: 4D flow cardiovascular magnetic resonance study, J. Cardiovasc Magn. Reson 24 (2022) 4, https://doi.org/10.1186/s12968-021-00832-2.
[28] Atsuko Kato, Eugénie Riesenkampff, Deane Yim, et al., Pediatric Fontan patients are at risk for myocardial fibrotic remodeling and dysfunction, Int J. Cardiol. 240 (2017) 172–177, https://doi.org/10.1016/j.ijcard.2017.04.073.
[29] T. Bharucha, R. Khan, L. Mertens, et al., Right ventricular mechanical dyssynchrony and asymmetric contraction in hypoplastic heart syndrome are associated with tricuspid regurgitation, J. Am. Soc. Echocardiogr. 26 (2013) 1214–1220, https://doi.org/10.1016/j.echo.2013.06.015.
[30] S.J. Zaidi, J. Penk, V.W. Cui, et al., Right ventricular mechanical dyssynchrony in hypoplastic left heart syndrome: correlation with systolic function and QRS duration, Pedia Cardiol. 40 (2019) 934–942, https://doi.org/10.1007/s00246-019-02091-6.
[31] J. Gokhale, N. Husain, L. Nicholson, et al., QRS duration and mechanical dyssynchrony correlations with right ventricular function after fontan procedure, J. Am. Soc. Echocardiogr. 26 (2013) 154–159, https://doi.org/10.1016/j.echo.2012.10.018.
[32] A. Rösner, T. Khalapyan, H. Dalen, et al., Classic-pattern dyssynchrony in adolescents and adults with a Fontan circulation, J. Am. Soc. Echocardiogr. 31 (2018) 211–219, https://doi.org/10.1016/j.echo.2017.10.018.
[33] M. Kanski, J. Töger, K. Steding-Ehrenborg, et al., Whole-heart four-dimensional flow can be acquired with preserved quality without respiratory gating, facilitating clinical use: a head-to-head comparison, BMC Med Imaging 15 (2015) 20, https://doi.org/10.1186/s12880-015-0061-4.